Second Annual Progress Report
for the Project

Laboratory Studies of Heterogeneous Chemical Processes of Atmospheric Importance

Supported under
NASA Grant Number:
NAG5-12707

Prepared for

UPPER ATMPOSPHERIC RESEARCH PROGRAM
NASA Headquarters
300 E Street, S.W.
Code YS
Washington, DC 20546-0001
Attn: Dr. Michael J. Kurylo, Program Manager

Principal Investigator:

Mario J. Molina
Massachusetts Institute of Technology
Room 54-1814
77 Massachusetts Avenue
Cambridge, MA 02139
Phone: (617) 253-5081; Fax: (617) 258-6525
E-mail: mmolina@mit.edu

LABORATORY STUDIES OF HETEROGENEOUS CHEMICAL PROCESSES OF ATMOSPHERIC IMPORTANCE

OBJECTIVE:

The objective of this study is to conduct measurements of chemical kinetics parameters for heterogeneous reactions of importance in the stratosphere and the troposphere. It involves the elucidation of the mechanism of the interaction of HCl vapor with ice surfaces, which is the first step in the heterogeneous chlorine activation processes, as well as the investigation of the atmospheric oxidation mechanism of soot particles emitted by biomass and fossil fuels. The techniques being employed include turbulent flow–chemical ionization mass spectrometry and optical ellipsometry, among others.

The next section summarizes our research activities during the second year of the project, and the section that follows consists of the statement of work for the third year.

ACCOMPLISHMENTS:

INTERACTION OF HCL WITH ICE SURFACES

Summary

We have continued our studies of the mechanism of the uptake of hydrogen chloride (HCl) on ice crystals. The initial results of the ellipsometry studies were summarized in the first progress report.

We have investigated the nature of the uptake on ice crystals of a non-polar species, namely CFC-12 (CF_2Cl_2). The results are surprising, and indicate that the ice crystal surface is modified on a time-scale of tens of minutes in the presence of CFC-12 at partial pressures corresponding to part-per-billion levels in the atmosphere. We have further probed the formation of the quasi-liquid layer (QLL) by following the course of the reaction of gaseous chlorine nitrate with ice exposed to HCl at partial pressures covering those relevant to stratospheric conditions. In particular, we monitor the formation of Cl_2, the reaction product, as chlorine nitrate also reacts directly with ice to form HOCl. There is a clear enhancement in the reaction rate as the QLL forms, indicating that the HCl in the QLL is ionized and readily available for surface reactions.

We have also investigated the uptake of acetic acid in the presence of HCl, and again the uptake is strongly influenced by the formation of the QLL. The experiment was designed to probe a change in the affinity of acetic acid molecules as the surface becomes more liquid-like; we conclude that QLL induces a stronger interaction of the acetic acid molecules with the surface, as expected from the increased mobility of the water molecules in the QLL and the polarity of the acetic acid molecules.

The results of these experiments are summarized in the attached manuscript, which we plan to submit in the near future, after some editorial changes:

Quasi-Liquid Layer Formation on Ice in the presence of HCl under Stratospheric Conditions. V. Faye McNeill, Thomas Loerting, Bernhardt L. Trout, Luisa T. Molina, Mario J. Molina. To be submitted to *Nature*.

ATMOSPHERIC OXIDATION OF SOOT

We have continued our investigations of the chemical properties of soot particles in order to elucidate their atmospheric chemical transformations. As before, we are utilizing methane soot as a proxy for tropospheric soot aerosol. The experiments were performed using a chemical ionization mass spectrometer (CIMS) combined with matrix isolation technique (MI) and coupled with a fast flow reactor at low (1-3 Torr) pressure and room temperature. Oxygen was used as the carrier gas.

Three types of experiments were conducted during the second phase of these studies

1. Kinetic study of OH uptake on methane soot including
   - Time dependence,
   - Dependence on initial concentrations of hydroxyl radicals,
   - Influence of relative humidity
   - Types of OH source used ($H+NO_2$, $H+O_2+M$, microwave discharge of water vapor);

2. Surface electric charge study in course of the OH-initiated oxidation of methane-soot surfaces;

3. Detection and identification of the products of methane-soot oxidation released to the gas phase and study of product distribution evolution in the presence of various gas-phase species (OH, H_2O, and NO_x).

As described in our first progress report, CIMS is very sensitive to OH radicals and has the detection limit of ~10^6 molecule cm^{-3} at S/N ratio of 20 with an integration time of 5 seconds.

Results

For reliability and reproducibility purposes, freshly prepared soot samples were conditioned by inserting them in the flow-tube at pressures of ~10^{-2} Torr for 1-2 days to remove water and gases formed and adsorbed during the soot generation process.

Kinetics studies:

The soot surface was exposed to [OH] = (1-3) $\cdot 10^8$ molecule cm^{-3} during 8-hr period. The OH uptake coefficient was measured every 30 minutes and was found to be $\geq$ 0.2, independent of the length of exposure time. This result shows that there is a high efficiency for the OH uptake by fresh or completely oxidized soot.

We also investigated how the OH uptake coefficient changes at various initial OH concentrations in the range from $2 \cdot 10^7$ to $9 \cdot 10^9$ molecule cm^{-3}. Within experimental error no change in the OH uptake coefficient was observed, even in the presence of NO_x. This finding confirms that the gas-phase chemistry of OH radicals is of minor importance in our laboratory apparatus.

The methane-soot samples were exposed as well to water vapor in the presence of [OH] = (1-2) $\cdot 10^8$ molecule cm^{-3}. The OH uptake coefficient was found to independent of relative humidity in the 0 to 6.4% range.

Surface charge

Since the soot surface is a good electric insulator and has a large specific surface area, it can be charged during its formation and keep its surface charge for long periods of time. We investigated if charged species can be formed and released to the gas phase during exposure of soot samples to OH. A noticeable imbalance of ion current from parent ions such H_3O^+ (mass 19) and $H_3O^+ * H_2O$ (mass 37) was detected when the movable OH source was placed in and out of contact with the soot samples. This difference in ion current indicates that some fraction of the gas phase species formed during oxidation can be charged. To confirm this experimental finding we detected directly the ionic current from the products of oxidation in the absence of parent ions. The observed irregular ion signals with relatively high intensity at several masses show that some of the oxidation products are charged. The quantification of this phenomenon requires using a specific surface-charge sensitive method.

Gas phase products

The gas-phase product distribution was studied using the matrix isolation-CIMS technique. The procedure was as follows: the soot samples were exposed to OH at concentration levels in the range from 2 to 100 $\cdot 10^7$ molecule cm^{-3} in the presence of O_2, NO_x and H_2O, and the gas-phase products were collected with a fingerlike quartz trap kept at liquid nitrogen temperature during approximately one hour. The trap was then

slowly warmed up by blowing small amounts of helium through the flow-tube, and the mass spectrum over the 10-250 mass range was continuously recorded for 30 minutes. The observed mass spectra were analyzed and the time dependencies of various masses were plotted. For identification purposes individual spectra of authentic samples were recorded to further compare with the spectra of the oxidation products. Among the identified products we found H_2O, HO_2, H_2O_2, CO, CO_2, HCO, CH_2O, HCOOH, C_6H_6, $C_6H_5CH_3$, $C_6H_5CH_2CH_3$, and $C_6H_5(CH_2)_2CH_3$. The actual product distribution includes other products that we have not yet identified. We believe that they are mostly aromatic radicals whose identification is very difficult, since it requires the use of specific reactions for their generation.

We also studied the product distribution as a function of the initial OH concentration, the relative humidity and the presence of NO_x. At a high OH concentration of ~10^9 molecule cm^{-3} the product distribution shifts toward low mass indicating a relatively intense oxidation of the soot surfaces with H_2O, H_2O_2, CO, and CO_2 as major products. At low OH concentrations more relevant to tropospheric conditions the product distribution is rich with high-mass products. It includes one-ring aromatic compounds with substitution groups of different lengths with a mass period of 14 (CH_2-). The influence of water on the product distribution is not completely understood yet because the sensitivity of the CIMS technique decreases in the presence of water vapor by forming clusters with parent ions as well product ions. A major effect of NO_x on the product distribution was found to be the additional formation of HONO and HNO_3, which has important atmospheric implications.

Conclusions

1. The results of the kinetic studies show the independence of the OH uptake by methane soot on (a) exposure time, (b) initial OH concentration and (c) water content (up to 6.4% relative humidity).

2. Charged species formed during the OH-initiated oxidation of methane-soot samples were detected indicating changes in the surface charge of soot particles.

3. The products released to the gas phase in the course of the heterogeneous oxidation of the methane soot surface were detected and many were identified. The observed product distribution changes depending on the gas-phase environment (presence of OH, H_2O and NO_x) and shows that the heterogeneous oxidation of soot surfaces is very efficient. These results are consistent with our previous studies on the OH-initiated oxidation of organic surfaces (alkane, aromatic and polyaromatic) and can be explained in terms of the reaction mechanism we proposed earlier for the oxidation of organic surfaces.

Carbon loss rates

The laboratory apparatus to investigate the rate of carbon loss of soot particles upon exposure to OH radicals has now been assembled and tested. The quartz microbalance

has been successfully coupled to a CIMS-fast flow reactor operating at pressures around 100 Torr; operation at one atmosphere will also be feasible.

STATEMENT OF WORK FOR THE THIRD YEAR OF THE PROJECT:

1. The interaction of HCl vapor with ice will continue to be investigated by completing the experimental flow-tube CIMS measurements and by conducting flow-tube modeling calculations to evaluate the suitability of various HCl uptake models, e.g. Langmuir adsorption, QLL, surface vs. bulk diffusion, etc.

2. Experimental OH uptake measurements will be conducted with the flow-tube CIMS technique utilizing soot generated in various ways, such as by burning hexane, diesel, wood, grass, etc. in order to investigate the behavior of actual atmospheric soot particles.

3. The fast flow-quartz crystal microbalance apparatus assembled in the second phase of the project will be employed to measure the carbon loss rate initiated by reaction of the OH radical with various soot samples as a function of oxygen pressure and relative humidity, to test the hypothesis that the atmospheric oxidation of soot leads to the release of significant amounts of volatile organic compounds to the gas phase under realistic atmospheric conditions.

Quasi-Liquid Layer Formation on Ice under Stratospheric Conditions

V. Faye McNeill, Thomas Loerting, Bernhardt L. Trout, Luisa T. Molina, Mario J. Molina

Massachusetts Institute of Technology, Cambridge, MA, USA 02139

Characterization of the interaction of hydrogen chloride (HCl) with ice is essential to understanding at a molecular level the processes responsible for ozone depletion[1,2] involving polar stratospheric cloud (PSC) particles. To explain the catalytic role PSC particle surfaces play during chlorine activation[2-5], we proposed previously that HCl induces the formation of a disordered region on the ice surface, a 'quasi-liquid layer' (QLL), at stratospheric conditions[6]. The QLL is known to exist in pure ice crystals at temperatures near the melting point, but its existence at stratospheric temperatures (-85 °C to -70°C) had not been reported yet[7-15]. We studied the interaction of HCl with ice under stratospheric conditions using the complementary approach of a) ellipsometry to directly monitor the ice surface, using chemical ionization mass spectrometry (CIMS) to monitor the gas phase species present in the ellipsometry experiments, and b) flow-tube experiments with CIMS detection. Here we show that trace amounts of HCl induce QLL formation at stratospheric temperatures, and that the QLL enhances the chlorine-activation reaction of HCl with chlorine nitrate ($ClONO_2$), and also enhances acetic acid (CH_3COOH) adsorption.

Surface disorder was observed via ellipsometry on pure single-crystalline hexagonal ice with no HCl present down to approximately -30 °C. This value is consistent with other experimentally determined values of QLL onset temperature for bare ice, which range from a few degrees below the melting point of water to less than -40 °C.[12-15]

Figure 1 summarizes the results of our investigation of the HCl-ice phase diagram using the ellipsometry-CIMS approach. A change in signal consistent with the formation of a disordered interfacial layer on the ice surface was observed in the range of HCl partial pressures and temperatures in the vicinity of the solid-liquid equilibrium line on the HCl-ice bulk phase diagram. It is important to note that this range of conditions includes those encountered in the polar stratosphere during PSC events. While surface disorder on ice at stratospheric conditions has been predicted theoretically,[16] this is the first report of experimental evidence of HCl-

induced QLL formation at stratospheric temperatures. Assuming the optical constants of this layer to be those of liquid water, we estimate that HCl induces a disordered layer with thicknesses of a few nanometers up to 100 nm depending on the quality of the ice-surface and the location in the phase-diagram.

In the range of HCl partial pressures and temperatures far from the solid-liquid equilibrium line, i.e. in the interior of the ice stability envelope, no surface change was observed. For example, exposure of an ice surface to approximately 10^{-7} Torr HCl was observed to induce QLL formation for T>-35°C and T<-65°C, but in the region -35 °C>T>-65°C we found no evidence of surface change. Indirect support for the observation that HCl-induced surface change is confined to the region of the HCl-ice phase diagram near the solid-liquid equilibrium line is found in the work of Hynes et al.,[17] who report that at 10^{-6} Torr HCl the uptake coefficient, γ, of HCl on ice decreased from $\gamma > 0.1$ at 200 K (conditions at which we observe surface change) to $\gamma < 0.01$ upon increasing the temperature above 205 K (conditions at which no surface change was observed in our experiment). Surface disorder is expected to enhance HCl uptake efficiency. Our flow tube-CIMS studies lend further support for the observed trend.

Two types of experiment were performed using the ellipsometer-CIMS system: a) constant temperature experiments in which the ice sample was exposed to a step change in partial pressure of HCl and the ellipsometer signal was monitored over time, and b) constant HCl partial pressures with temperature scanning experiments. Ellipsometer signal time traces for a typical temperature scanning experiment are shown in Figure 2. In the constant temperature experiments, after exposure to HCl, surface change was observed only after an induction time of 1-10 min. An aging effect was observed in that induction times were seen to decrease after the first exposure of a surface to HCl. Both the surface disordering and this aging effect were seen to be reversible.

The reaction of $ClONO_2$ with adsorbed HCl was studied using the flow tube-CIMS technique on zone-refined ice cylinders. As shown in Figure 3, the production of Cl_2, and thus the efficiency of the reaction, decreased as we moved from conditions where surface change was observed with the ellipsometer to those where no surface change was observed. At -77 °C, the reaction proceeds efficiently ($\gamma > 0.1$), and HCl is readily available on the surface for reaction, as has been observed previously.[2-5] At -55 °C, with the same reactant concentrations, HCl is not readily available on the surface for reaction, despite the gas-phase presence of HCl. Cl_2

evolution consists of an initial 'burst' followed by tailing off of Cl_2 release. Kinetic analysis of the 'burst' portion of the Cl_2 signal yields a reactive uptake coefficient at least one order of magnitude smaller ($\gamma = 0.014 +/- 0.005$) than that for the same reaction at temperatures where surface change was observed using ellipsometry.

The results of our flow tube-CIMS studies of HCl adsorption on zone refined ice cylinders, as shown in Figure 4, demonstrate that the nature of HCl adsorption on ice differs at the conditions under which surface change was observed with ellipsometry from the HCl-ice interaction at conditions under which no surface change was observed. At -77 °C and $7.4 \cdot 10^{-7}$ Torr HCl, almost fully reversible uptake was observed. An initial fast uptake mode ($\sim 10^{14}$ molecule cm^{-2} over 180 sec) was observed, which we attribute to surface adsorption prior to QLL formation. A second adsorption mode was observed consisting of a nearly constant flux of HCl ($\sim 5 \cdot 10^{11}$ molecules $cm^{-2} s^{-1}$) from the surface to the interior of the ice sample, which persisted throughout the time scale of the experiment (1 hour). This loss is observed to be reversible. A memory effect was observed in that this flux increased in magnitude with subsequent exposures of the same ice crystal. These observations of surface-to-bulk loss[18,19] and memory effect[4,17-19] are consistent with the findings of other investigators. A model of HCl absorbing into a 100 nm thick film with desorption properties between those of ice and liquid water, with diffusion from the near-surface region into the bulk ice lattice using $D_{HCl} = 10^{-12}$ $cm^2 s^{-1}$,[20] is sufficient to simulate the observed surface-to-bulk loss at long times. In addition, the $ClONO_2$ + HCl reactive uptake experiments indicate that this HCl is readily available for reaction with $ClONO_2$. Therefore, we attribute this loss mainly to absorption of HCl by the disordered surface region.

In flow tube-CIMS studies of HCl uptake at -59 °C and $6.5 \cdot 10^{-7}$ Torr HCl, conditions under which no surface change was observed with ellipsometry, we observed largely irreversible uptake. We again observed an initial fast mode of HCl adsorption ($\sim 6 \cdot 10^{14}$ molecules cm^{-2} over 500 sec), followed by a slower uptake mode, which leads to saturation within ~ 3000 sec. The magnitude of adsorbed HCl decreases with subsequent exposures but adsorption remains largely irreversible. The $ClONO_2$ + HCl reactive uptake experiments indicate that HCl adsorbed under these conditions is for the most part *not* readily available on the surface for reaction with $ClONO_2$. We attribute this irreversibly adsorbed, inaccessible HCl to diffusion into the bulk and into grain boundaries.

As a third corroboration of these findings, the co-adsorption of HCl and CH_3COOH was studied on zone-refined ice cylinders. CH_3COOH is a weak acid that does not dissociate on bare ice surfaces at -45 °C. [21] At a constant temperature of -61 °C, at partial pressures of HCl where no surface change was observed with ellipsometry ($P_{HCl} = 7 \cdot 10^{-7}$ Torr), an uptake of $\sim 1.4 \cdot 10^{14}$ molecule·cm^{-2} was observed. This is an overall enhancement compared to values of acetic acid uptake on bare ice, indicating that the presence of HCl enhances the affinity of acetic acid for the ice surface even when no surface change is observed via ellipsometry. At the same temperature, twofold enhancement in CH_3COOH adsorption ($2.9 \cdot 10^{14}$ molecule·cm^{-2}) was observed at higher HCl concentrations where surface disorder was observed ($P_{HCl} = 2 \cdot 10^{-6}$ Torr).

In conclusion, we have confirmed that surface disorder induced by the presence of HCl explains the role played by type II PSC particles in catalyzing chlorine activation reactions. This surface disorder also enhances the adsorption of species that do not participate in chlorine activation including weakly polar ones such as CH_3COOH. In the case of warmer temperature atmospheric ice particles, such as those encountered in tropospheric cirrus clouds, surface disorder may play a key role in surface chemistry. The affinity of gas phase adsorbates for these ice surfaces may be greater than previously assumed, with implications for the role of ice particles in the scavenging of semi-volatile gas phase species and the reactive heterogeneous chemistry of the troposphere.[22, 23]

METHODS

Ellipsometer-CIMS experiments

The ellipsometer used in these measurements (Beaglehole Instruments) employs a photoelastic birefringence modulator, allowing high sensitivity measurements. The light source is a 50 mW He/Ne laser, focused to a diameter of approximately 1 mm. We observe true melting at 0 °C, and do not see surface disorder far from the solid-liquid equilibrium line in the HCl-ice phase diagram, and therefore we infer that the laser does not melt the ice surface due to local heating. The ice sample was placed in an aluminum sample holder and housed in a vacuum-jacketed flow tube fitted with quartz windows to allow the laser beam to pass through the cooling jacket and flow tube walls. The flow tube was operated in the laminar flow regime ($Re < 100$) with He as a carrier gas. Ice was placed upstream of the main ice sample to ensure that the

sample was in equilibrium with water vapor, i.e. no net evaporation or condensation took place. The flow tube was interfaced with a CIMS apparatus (Extrel C50) to monitor the gas phase composition via chemical ionization by SF_6^- reagent ions. HCl was monitored as SF_5Cl^- (162 amu). In an HCl uptake experiment, the ice sample was exposed to a dilute mixture of HCl in He that was introduced to the main He flow through a moveable injector positioned near the centerline of the flow tube. The injector was heated to prevent experimental artifacts due to adsorption of HCl to the injector walls, creating a temperature gradient of < 1°C in the flow tube. Ice samples were prepared from single crystals of ice grown using an adaptation of the Bridgeman technique[24] and were observed using crossed polaroids to have grain sizes on the order of centimeters.

Flow tube-CIMS experiments

All flow tube-CIMS experiments employed a 2.5 cm i.d. flow tube operating in the laminar flow regime (Re < 100) that was interfaced with a CIMS apparatus (Extrel C50). Detection occurred via SF_6^-. HCl was monitored as SF_5Cl^- (162 amu), $ClONO_2$ was monitored as $ClONO_2F^-$ (116 amu), Cl_2 was monitored as Cl_2^- (70 amu), and CH_3COOH was monitored as $CH_3CO_2HF^-$ (79 amu).

Hollow cylindrical ice samples ~ 2 mm thick were prepared using a modification of the Bridgeman technique,[24] using a cylindrical mask to form the central flow channel. Ice samples formed in this way were observed using crossed polaroids to have grain sizes on the order of several millimeters.

In an HCl uptake experiment, the ice sample was exposed to HCl via a heated injector as in the ellipsometry-CIMS experiments. The $ClONO_2$ + HCl experiments and the acetic acid/HCl co-adsorption experiments employed two injectors.

In the $ClONO_2$ + HCl experiments, first a constant flow of HCl was established. Once the surface was saturated with HCl, the uptake of a constant flow of $ClONO_2$ and the associated Cl_2 evolution was monitored. $ClONO_2$ was prepared from ClF and $Pb(NO_3)_2$ using the method of Schmeisser[25] followed by fractional distillation at -77 °C and -95 °C, producing a high-purity sample. Reactive uptake measurements at several exposed ice lengths (and thus reaction times) were converted into kinetic information using the Brown algorithm.[26] Values reported here were calculated using a $ClONO_2$ diffusion coefficient in He of 176 cm^2sec^{-1}Torr at 200K, assuming a

$T^{1.76}$ dependence.[27] Reported uncertainties reflect a 20% uncertainty in diffusion coefficient and the observed loss rates.

In the acetic acid/HCl co-adsorption experiments, initailly a constant flow of HCl was established. Once the surface was saturated with HCl, the uptake of a constant flow of CH_3COOH and the associated HCl desorption was monitored. Dimerization of gas-phase acetic acid was accounted for when determining the acetic acid sample concentration and thus the partial pressure of acetic acid in the flow tube. The equilibrium constant for dimerization at 25 C and 1 atm is 0.972.[28]

FIGURES

Figure 1. The phase-diagram of HCl-ice adapted from Molina et al.[6] Thermodynamically stable phases are shown as a function of temperature and HCl partial pressure.[6,29] "Ice" is the stable phase under polar stratospheric conditions (circled area). "Liquid" refers to a liquid solution, and "Trihydrate" and "Hexahydrate" refer to the crystalline hydrate states. Note that, experimentally, the phase transitions might be observed with a delay due to kinetic barriers. Circles (o) refer to conditions where a change in signal consistent with the formation of a disordered interfacial layer on the ice surface was observed upon exposure of the ice crystal to HCl, whereas filled boxes (■) refer to conditions where no change to the ice surface was observed. Arrows represent experiments involving a scan in temperature during exposure to a constant partial pressure of HCl. Bars represent temperatures at which we observe cease/onset of surface changes. Transition to the hexahydrate phase or the melt is indicated by "Δ".

Figure 2. Time study of phase-modulated ellipsometry signal for ice sample exposed to $5 \cdot 10^{-7}$ Torr HCl and temperatures ranging from –52.5 °C to -77.2 °C. The traces shown are the ellipsometer signals measured at 50 kHz (x-trace) and 100 kHz (y-trace). The x- and y- traces are related to the real and the imaginary-part of the reflectivity, respectively. The ice sample was held initially at –52.5 °C, cooled to -77.2 °C, and then warmed again to –52.5 °C. As the temperature decreases, there is a discontinuity in the signals corresponding to a surface change at -66.5 °C. When the sample is then warmed to its original temperature, another discontinuity is observed, with the signals returning to their previous levels at -64.5 °C. Experiments such as this one are labeled using arrows in Figure 1.

Figure 3. The reaction of $ClONO_2$ with adsorbed HCl on zone-refined ice cylinders. Experiments shown were conducted at approximately $1 \cdot 10^{-6}$ Torr HCl and $5 \cdot 10^{-7}$ Torr $ClONO_2$ (pseudo-first order conditions). The left and right panels show studies of the reaction at -56 °C and -77 °C, respectively, and the upper and lower panels show $ClONO_2$ and Cl_2 mass spectrometer signals, respectively. The production rate of Cl_2 --and thus the efficiency of the reaction-- decreases as we move from conditions where surface change was observed with the ellipsometer to those where no surface change was observed.

Figure 4. HCl adsorption on zone-refined ice at approximately $7 \cdot 10^{-7}$ Torr HCl. The upper and lower traces are HCl mass spectrometer signal for adsorption at -77 °C and -59 °C, respectively. The nature of the interaction of HCl with the ice samples changes as we move from conditions where surface change was observed with the ellipsometer to those where no surface change was observed.

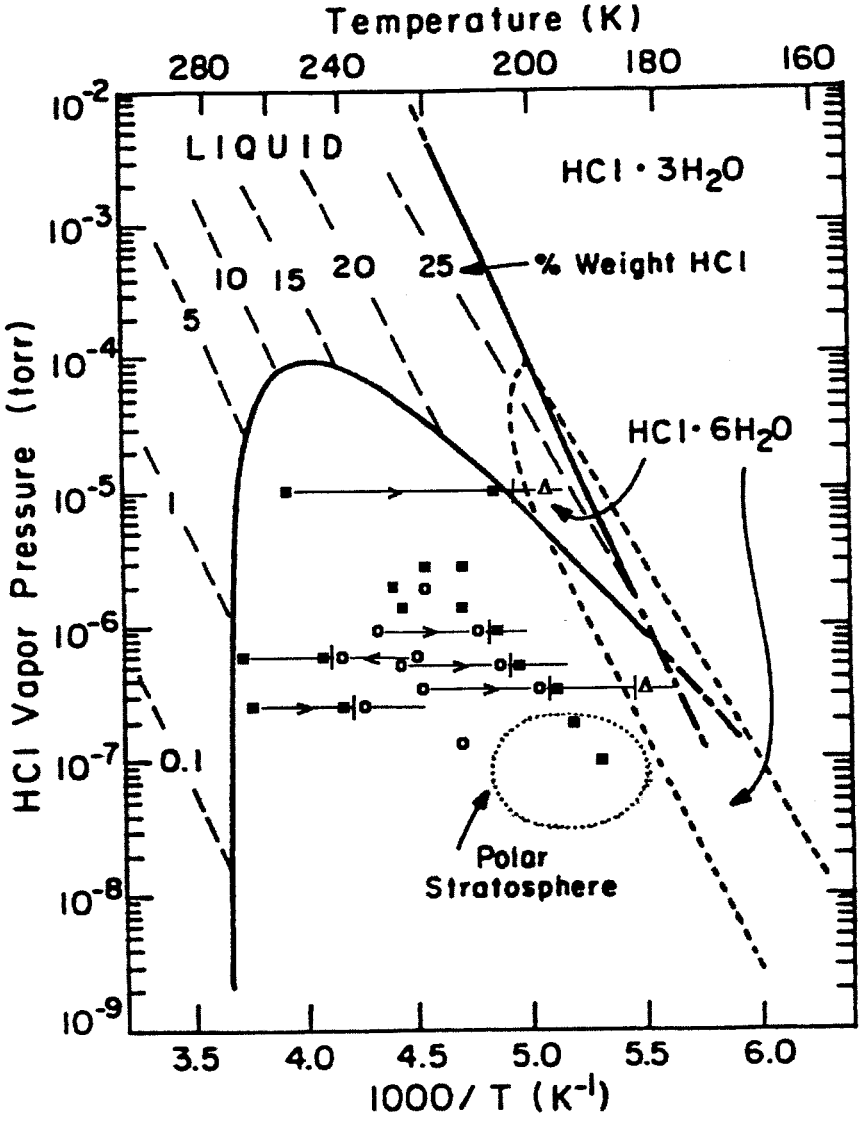
Temperature (K)
280
240
200
180
160
LIQUID
HCl · 3H2O
% Weight HCl
5
10
15
20
25
HCl · 6H2O
1
0.1
Polar
Stratosphere
HCl Vapor Pressure (torr)
10-2
10-3
10-4
10-5
10-6
10-7
10-8
10-9
3.5
4.0
4.5
5.0
5.5
6.0
1000/ T (K-1)

Figure 1.

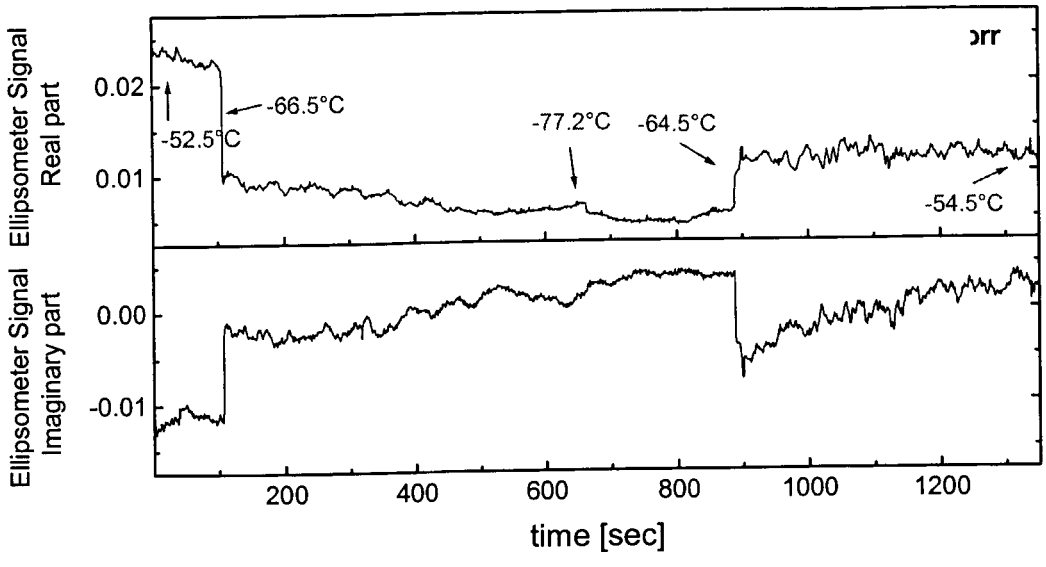

Figure 2.

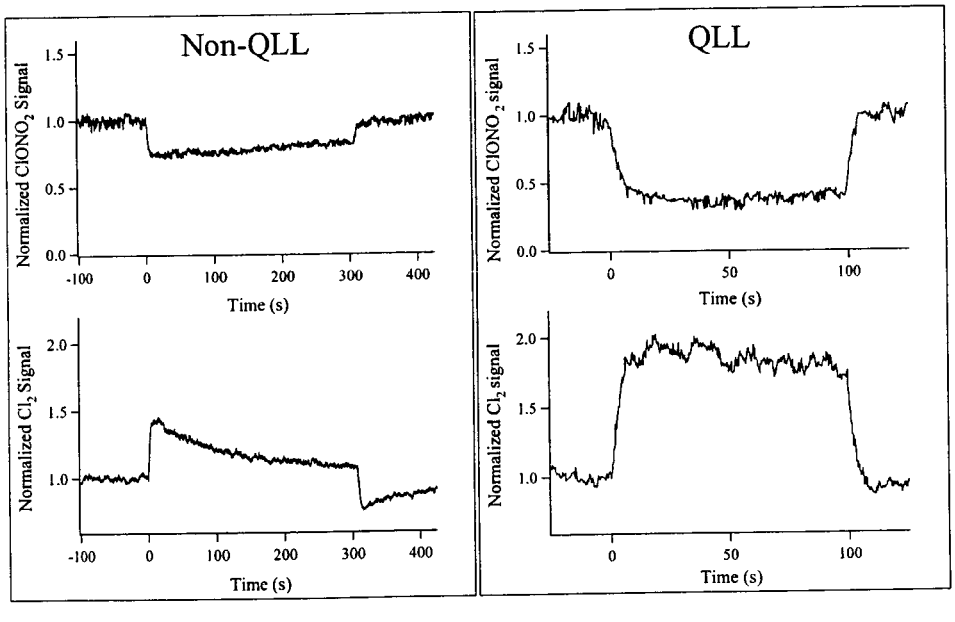

Figure 3.

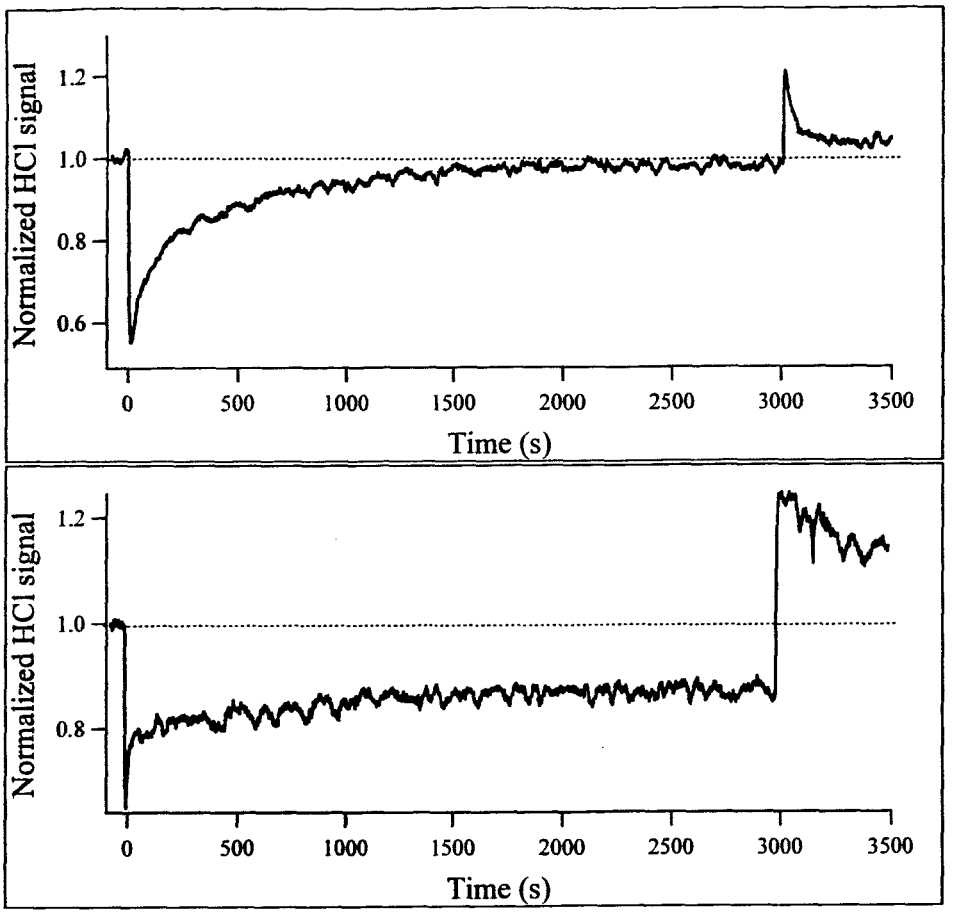
Normalized HCl signal
1.2
1.0
0.8
0.6
0
500
1000
1500
2000
2500
3000
3500
Time (s)
Normalized HCl signal
1.2
1.0
0.8
0
500
1000
1500
2000
2500
3000
3500
Time (s)

Figure 4.

REFERENCES

1. Solomon,S., Garcia,R.R., Rowland,F.S. & Wuebbles,D.J. On the Depletion of Antarctic Ozone. *Nature* **321**, 755-758 (1986).
2. Molina,M.J., Tso,T.L., Molina,L.T. & Wang,F.C.Y. Antarctic Stratospheric Chemistry of Chlorine Nitrate, Hydrogen Chloride and Ice - Release of Active Chlorine. *Science* **238**, 1253-1257 (1987).
3. Leu,M.T. Laboratory Studies of Sticking Coefficients and Heterogeneous Reactions Important in the Antarctic Stratosphere. *Geophysical Research Letters* **15**, 17-20 (1988).
4. Hanson,D.R. & Ravishankara,A.R. Investigation of the Reactive and Nonreactive Processes Involving $ClONO_2$ and HCl on Water and Nitric-Acid Doped Ice. *Journal of Physical Chemistry* **96**, 2682-2691 (1992).
5. Chu,L.T., Leu,M.T. & Keyser,L.F. Heterogeneous Reactions of HOCl+HCl $\rightarrow$ Cl_2+H_2O and $ClONO_2$+HCl $\rightarrow$ Cl_2+HNO_3 on Ice Surfaces at Polar Stratospheric Conditions. *Journal of Physical Chemistry* **97**, 12798-12804 (1993).
6. Molina,M.J. The Chemistry of the Atmosphere: The Impact of Global Change. Calvert,J.G. (ed.), pp. 27-38 (Blackwell Sci. Publ., Boston,1994).
7. Petrenko,V.F. & Whitworth,R.W. Physics of Ice. Oxford University Press, New York (1999).
8. Dash,J.G., Fu,H. & Wettlaufer,J.S. The premelting of ice and its environmental consequences. *Rep. Prog. Phys.* **58**, 115-67 (1995).
9. Toubin,C. *et al.* Dynamics of Ice Layers Deposited on MgO(001): Quasielastic Neutron Scattering Experiments and Molecular Dynamics Simulations. *Journal of Chemical Physics* **114**, 6371-6381 (2001).
10. Demirdjian,B. *et al.* Structure and dynamics of ice I_h films upon HCl adsorption between 190 and 270 K. I. Neutron diffraction and quasielastic neutron scattering experiments. *J. Chem. Phys.* **116**, 5143-5149 (2002).
11. Geiger,F.M., Tridico,A.C. & Hicks,J.M. Second Harmonic Generation Studies of Ozone Depletion Reactions on Ice Surfaces under Stratospheric Conditions. *Journal of Physical Chemistry B* **103**, 8205-8215 (1999).
12. Mizuno,Y. & Hanafusa,N. Studies of Surface-Properties of Ice Using Nuclear-Magnetic-Resonance. *Journal De Physique* **48**, 511-517 (1987).
13. Doeppenschmidt,A. & Butt,H.-J. Measuring the Thickness of the Liquid-like Layer on Ice Surfaces with Atomic Force Microscopy. *Langmuir* **16**, 6709-6714 (2000).
14. Sadtchenko,V. & Ewing,G.E. Interfacial melting of thin ice films: An infrared study. *Journal of Chemical Physics* **116**, 4686-4697 (2002).
15. Bluhm,H., Ogletree,D.F., Fadley,C.S., Hussain,Z. & Salmeron,M. The premelting of ice studied with photoelectron spectroscopy. *J. Phys. : Cond. Matter* **14**, L227-L233 (2002).

16. Mantz,Y.A., Geiger,F.M., Molina,L.T., Molina,M.J. & Trout,B.L. First-Principles Theoretical Study of Molecular HCl Adsorption on a Hexagonal Ice (0001) Surface. *J. Phys. Chem. A* **105**, 7037-7046 (2001).

17. Hynes,R.G., Mossinger,J.C. & Cox,R.A. The Interaction of HCl With Water-ice at Tropospheric Temperatures. *Geophysical Research Letters* **28**, 2827-2830 (2001).

18. Fluckiger,B., Chaix,L. & Rossi,M.J. Properties of the HCl/ice, HBr/ice, and H_2O/ice interface at stratospheric temperatures (200 K) and its importance for atmospheric heterogeneous reactions. *Journal of Physical Chemistry A* **104**, 11739-11750 (2000).

19. Huthwelker,T., Malmstrom,M.E., Helleis,F., Moortgat,G.K. & Peter,T. Kinetics of HCl uptake on ice at 190 and 203 K: implications for the microphysics of the uptake process. *Journal of Physical Chemistry A* **108**, 6302-6318 (2004).

20. Thibert,E. & Domine,F. Thermodynamics and Kinetics of the Solid Solution of HCl in Ice. *J. Phys. Chem. B* **101**, 3554-3565 (1997).

21. Sokolov,O. & Abbatt,J.P.D. Adsorption to ice of n-alcohols (ethanol to 1-hexanol), acetic acid, and hexanal. *J. Phys. Chem. A* **106**, 775-782 (2002).

22. Abbatt,J.P.D. Interactions of atmospheric trace gases with ice surfaces: Adsorption and reaction. *Chemical Reviews* **103**, 4783-4800 (2003).

23. Baker,M.B. Cloud microphysics and climate. *Science* **276**, 1072-1078 (1997).

24. Ohtomo,M., Ahmad,S. & Whitworth,R.W. A technique for the growth of high quality single crystals of ice. *J. Phys. , Colloq.* 1-595 (1987).

25. Schmeisser,M., Eckermann,W., Gundlach,K.P. & Naumann,D. New Methods for the Preparation of Chlorine Nitrate $ClONO_2$. *Zeitschrift fur Naturforschung Section B-A Journal of Chemical Sciences* **35**, 1143-1145 (1980).

26. Brown,R.L. Tubular Flow Reactors with 1st-Order Kinetics. *Journal of Research of the National Bureau of Standards* **83**, 1-8 (1978).

27. Hanson,D.R. & Ravishankara,A.R. The Reaction Probabilities of $ClONO_2$ and N_2O_5 on Polar Stratospheric Cloud Materials. *Journal of Geophysical Research-Atmospheres* **96**, 5081-5090 (1991).

28. Chao,J. & Zwolinski,B.J. Ideal-Gas Thermodynamic Properties of Methanoic and Ethanoic Acids. *Journal of Physical and Chemical Reference Data* **7**, 363-377 (1978).

29. Hanson,D.R. & Mauersberger,K. Hydrogen chloride/water solid-phase vapor pressures and hydrogen chloride solubility in ice. *J. Phys. Chem.* **94**, 4700-5 (1990).